Winter 12-24-2014

An Inductive Sensor for Real Time Measurement of Plantar Normal and Shear Forces Distribution

Li Du
The University of Akron, Main Campus

X Zhu

J. Zhe

This article has been accepted for publication in a future issue of this journal, but has not been fully edited. Content may change prior to final publication. Citation information: DOI 10.1109/TBME.2014.2386136, IEEE Transactions on Biomedical Engineering

An Inductive Sensor for Real Time Measurement of Plantar Normal and Shear Forces Distribution

Li Du, Xiaoliang Zhu, and Jiang Zhe*

Abstract*—*Goal: **The objective of this article is to demonstrate a multiplexed inductive force sensor for simultaneously measuring normal force and shear forces on a foot.** ***Methods:*** **The sensor measures the normal force and shear forces by monitoring the inductance changes of three planar sensing coils. Resonance frequency division multiplexing was applied to signals from the multiple sensing coils, making it feasible to simultaneously measure the three forces (normal force, shear forces in x and y axis) on a foot using only one set of measurement electronics with high sensitivity and resolution.** ***Results:*** **The testing results of the prototype sensor have shown that the sensor is capable of measuring normal force ranging from 0 to 800 N and shear forces ranging from 0 to 130 N in real time.** ***Conclusion:*** **With its high resolution, high sensitivity and the capability of monitoring forces at different positions of a foot simultaneously, this sensor can be potentially used for real time measurement of plantar normal force and shear forces distribution on diabetes patient's foot.** ***Significance:*** **Real time monitoring of the normal force and shear forces on diabetes patient's foot can provide useful information for physicians and diabetes patients to take actions in preventing foot ulceration.**

***Index Terms*— Foot ulcer monitoring, inductive sensor, plantar normal force, plantar shear forces.**

I. Introduction

OVER 8% of adults population in the world is suffering from diabetes as of 2013, and this number could reach 11% by 2035 [1]. Up to 20% of diabetes patients will develop foot ulcerations and 85% of foot amputations are related to diabetes caused foot ulcerations [2]. Although the causing of the foot ulceration is not fully understood, recent studies show that excessive normal force and shear forces generated on the plantar surface significantly contribute to foot ulceration [2-4]. Therefore monitoring the normal force and shear forces on diabetes patient's feet in real time can provide useful information for physicians and diabetes patients to take actions to prevent the foot ulceration [5-8]. For instance, this information can help the physicians to prescribe a preventive course of actions or advise the patients to correct their walking habits.

A variety of measurement systems were developed to detect forces on patients' foot. Load sensors and pressure sensors have been used for foot stress measurement due to its simple structure and low cost [9-12]. For instance, to measure the plantar pressure distribution, F-Scan® and Pedar® systems were developed using a pressure sensor array. Although these measurement systems are sensitive to normal force, they cannot measure shear forces. To overcome this problem, shear sensors were integrated with F-Scan® pressure distribution sensor sheet into an insole [13]. However, the use of the high cost F-Scan® makes it unaffordable for many diabetes patients [13]. To reduce the cost, Perry et al reported the use of strain gauges array to accurately detect normal force and shear forces at the same time [14]. Because of the bulky size, a patient has to stand on the sensor array to measure the forces on the plantar surface; it is therefore unsuitable for real time monitoring of foot forces and ulceration.

A miniature sensor based on loop antenna was reported in [15], the resonant frequency of the loop antenna shifted as the foot forces are applied. Normal force and shear forces can be obtained by the natural frequency shifts with high resolution. However, the sensor is based upon capacitance change measurement, which is sensitive to environmental changes, such as changes in temperature or humidity. Additionally, the sensor was operated at around 5 GHz, and thus required complicated measurement electronics and data acquisition system for real-time applications. The sensor presented in Reference [16] consists of one excitation coil and three sensing coils embedded in a rubber element. Normal force and shear forces can be calculated from the voltage induced in the three sensing coils. The drawback of this sensor is that each sensing coil is sensitive to both normal force and shear forces, which makes it difficult to deduce the individual force components from three induced voltages. In addition, there was no dynamic testing reported in both references. A detailed review of plantar force measurement systems can be found in [17].

To overcome the above limitations, in this article we report a low cost, high sensitivity inductive force sensor for real time measurement of normal force and shear force on a foot. The presented foot force sensor consists of multiple mini-sized spiral planar coils as sensing elements; resonance-frequency division signal multiplexing was applied to the sensing coils, enabling simultaneous measurements of normal force and two

Manuscript received August 14, 2014; revised November 07, 2014 and December 15, 2014; accepted December 19, 2014. This work was supported by the University of Akron.

Li Du (ld22@zips.uakron.edu) and Xiaoliang Zhu (xz31@zips.uakron.edu) are with Mechanical Engineering, University of Akron, Akron, OH, 44325, USA. Jiang Zhe*, the corresponding author, is with Mechanical Engineering, University of Akron, Akron, OH, 44325, USA. (Correspondence e-mail: jzhe@uakron.edu).

This article has been accepted for publication in a future issue of this journal, but has not been fully edited. Content may change prior to final publication. Citation information: DOI 10.1109/TBME.2014.2386136, IEEE Transactions on Biomedical Engineering

axis shear forces using only one set of measurement electronics, with high sensitivity. The sensor, with further reduced size, can be potentially embedded in the shoe of a diabetes patient for real time plantar force monitoring.

II. Device Design and Sensing Mechanism

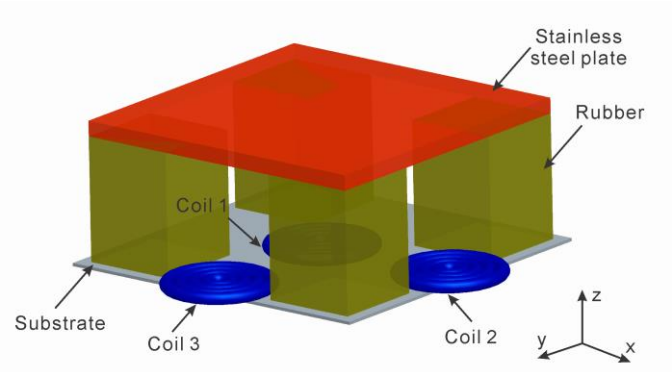

Fig. 1. Schematic of a three-coil inductive force sensor for foot ulcer monitoring.

Fig. 1 illustrates the design concept of a multiplexed inductive force sensor, consisting of three mini-sized spiral coils mounted on a square substrate, four Neoprene rubber blocks fixed at the four corners of the substrate, and a stainless steel plate mounted on the top of the rubber blocks. Coil 1 is attached at the center of the substrate. Coil 2 and coil 3 are positioned at the centers of two adjacent edges of the substrate separately. The small-size force sensor is to be embedded in the shoe of a diabetes patient for real time force measurement.

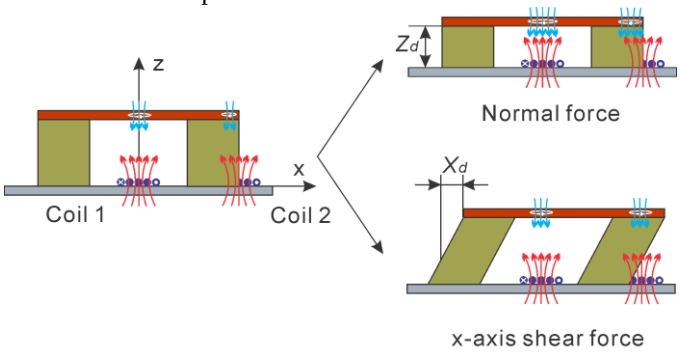

Fig. 2. Sensing mechanism of the three-coil inductive force sensor.

The working mechanism of the inductive force sensor is shown in Fig. 2. An AC excitation is applied to each sensing coil to generate a magnetic field (red line with up arrows in Fig. 2); an eddy current is induced inside the stainless steel plate, which generates an opposite magnetic field (light blue line with down arrows in Fig. 2) and causes a decrease in the coil's inductance L_s. The decrease of L_s is a function of the following two factors: 1) the vertical distance Z_d between the coil plane and the stainless steel plate; the smaller the Z_d, the larger the eddy current and therefore the larger the drop in the inductance L_s, 2) the volume of the stainless steel plate within the magnetic field generated by a coil; the larger the volume of stainless plate within the magnetic field, the larger the decrease in L_s of this coil. When a normal force is applied on the top plate, the rubber blocks are compressed and Z_d decreases, leading to a decrease on L_{s1}. Shear forces in x and y direction, on the other hand, cause displacement of the stainless plate along x and y direction (Z_x and Z_y), and affect the inductance of coil 2 and 3 respectively. However, L_{s1} is not affected by shear forces because the displacement would not affect the eddy current generated by coil 1. Therefore the normal force on the foot can be obtained by solely monitoring the inductance change of coils 1 (ΔL_{s1}). The inductance change of coil 2 (ΔL_{s2}) is a function of both normal force and x-axis shear force. Once normal force is obtained from ΔL_{s1}, x-axis shear force can be recovered from ΔL_{s2}. Similarly, the inductance change of coil 3 (ΔL_{s3}) is a function of both normal force and y-axis shear force; the y-axis force can be recovered from ΔL_{s3}.

To accurately acquire the peak forces at critical positions including toes, metatarsal heads (MTH) and heel, the optimal sensing area of the sensor was found to be around 25.4 mm by 25.4 mm [3]. Hence we determined the length and width of the stainless steel plate to be 25.4 mm. For a person with ordinary weight, the normal force and shear forces generated during walking could reach 800 N and 130 N, respectively [3]. To withstand the high normal force a stainless steel plate with 1 mm thickness was selected to build the prototype sensor. Four rubber blocks (10 mm (Length)×10 mm (Width)×10 mm (Height)) with durometer hardness 40A were used to obtain linear deformation by forces ranging from 0 to 800 N. Each planar coil was designed to be 10 mm in outer diameter and 0.8 mm in inner diameter. Such a design ensures the coil is sensitive to the Z_d up to 10 mm [18]. We tested magnet wires with different diameters and found that a wire with 0.2 mm in diameter generated the highest sensitivity. After the three 22-turn sensing coils were built, the series resistance R_s and series inductance L_s were measured to be around 1.53 Ω and 2.70 μH by a high precision LCR meter. With an excitation frequency of 2 MHz, the Q factor of the sensing coil was calculated to be around 16.2. The coupling coefficient k between three coils was ranged from 0.001 to 0.007 at 2 MHz, which indicates the mutual interference between three sensing coils is negligible.

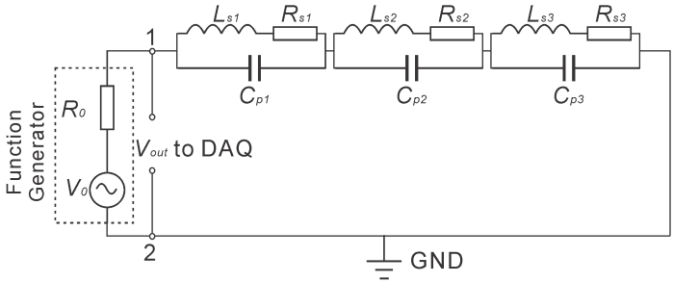

Fig. 3. Equivalent measurement circuit for a three-coil foot force sensor.

Fig. 3 shows the measurement circuit for the inductive force sensor with three sensing coils. L_{si} and R_{si} (i=1, 2, 3) represent the series inductance and resistance for each sensing coil. Each sensing coil is electrically connected in parallel with an external capacitor C_{pi} (i=1, 2, 3) to form a parallel LC resonant circuit that has a unique resonant frequency. A combined excitation signal (V_0) consisting of three sine waves whose frequencies are

This article has been accepted for publication in a future issue of this journal, but has not been fully edited. Content may change prior to final publication. Citation information: DOI 10.1109/TBME.2014.2386136, IEEE Transactions on Biomedical Engineering

close to the resonant frequencies of the three LC resonant circuits is applied. Only one combined response V_{out} is measured. Because signals from each sensing coil exhibit a peak amplitude at its resonant frequency, the signals for each individual channel can be recovered from the combined response by taking the spectrum components at each resonant frequency. Inductance change for each sensing coil can therefore be calculated from individual signals. More details about resonant frequency division multiplexing techniques can be found in [19, 20]. From the measured inductance changes, foot forces can be back calculated from calibration curves. Excitation frequencies for the three sensing coils were experimentally determined to be 1.51 MHz, 1.76 MHz and 1.95 MHz. More detailed procedures of measurement parameter determination for applying resonant frequency division multiplexing can be found in reference [19].

III. Experimental Results and Discussions

A. Calibration

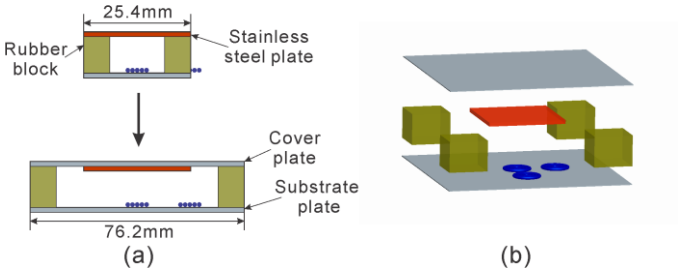

Fig. 4. Schematic of a modified prototype foot force sensor for calibration and testing.

To acquire accurate relationship between applied force and inductance changes of sensing coils, calibrations for the three sensing coils were conducted at different normal forces and shear forces. Note that the dimension of the designed sensor shown in Fig. 1 is 25.4 mm (Length)×25.4 mm (Width)×16 mm (Height). The small size makes it difficult to apply known normal and shear forces by the hydraulic cylinders to evaluate the sensor's response and to conduct the dynamic testing. To facilitate the calibration and dynamic testing, we fabricated a modified prototype sensor (shown in Fig. 4) with a larger substrate plate (76.2 mm×76.2 mm area with a thickness of 3mm) made of PMMA; the dimensions of the sensing coils, stainless steel plate and rubber block all remained the same. The responses of the 25.4 mm×25.4 mm and 76.2 mm×76.2 mm sensor should be exactly the same. Four rubber blocks were fixed at the four corners of the substrate by applying a small amount of super glue. The 25.4 mm×25.4 mm stainless steel plate was attached to center of a cover plate with the same size of the substrate plate (76.2 mm×76.2 mm); next the cover plate was fixed on top of the rubber blocks to finish the fabrication of the prototype sensor.

Fig. 5 illustrates the calibration setup for the prototype sensor. The calibration system consists of two hydraulic cylinders, two nitrogen cylinders, a ball bearing linear translation stage, a function generator and a high speed DAQ system. First a mounting block (black component in Fig. 5) was installed on the damped optical table (RS2000TM, Newport). Next the substrate plate of the modified prototype sensor shown in Fig. 4 was attached to the PMMA mounting plate using mounting tape. Then the cover plate of the prototype sensor was attached to a ball bearing linear translation stage (Oriel 16021 ball bearing linear stage, HOFSTRA group, the purple component in Fig. 5) to ensure the direction of the applied shear force is perpendicular to the direction of normal force. The other side of the linear translation stage was connected to hydraulic cylinder #1 via thread end of the piston. Hydraulic cylinder #1 (NCDGBN32-0400 Air Cylinder, SMC PNEUMATICS) was used to simulate normal force along z direction, hydraulic cylinder #2 was used to apply shear forces along x direction (or y direction). The generated force can be calculated by $F=P\times A$, in which P is the pressure readout from the pressure gauge and A is the bore area of the hydraulic cylinder. The bore size of the hydraulic cylinder is 32 mm. Forces applied by hydraulic cylinders can be controlled by regulating the output of two nitrogen cylinders. For instance, the applied force generated by a 6.90 kPa pressure is 55.45 N. The actual normal force and shear forces applied by the two cylinders were measured and calibrated by a precision digital scale with a resolution of 1 N. Note that the normal force applied by cylinder 1 may result in resistance for shear movement along x-axis and y-axis. However, the linear translation stage utilized in the tests was well lubricated to minimize the movement resistance. The resistance caused by the linear translation stage was negligible comparing to the applied shear forces. The responses of three sensing coils were measured using the DAQ system.

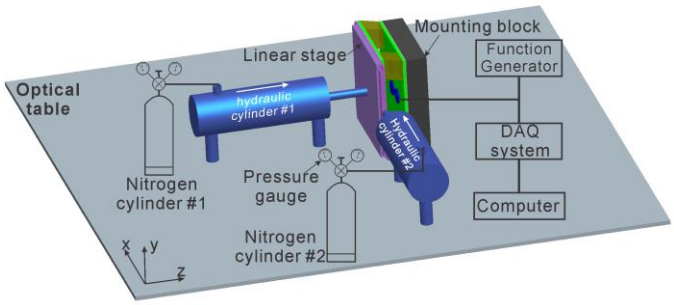

Fig. 5. Experimental setup for the prototype foot force sensor calibration.

The calibration was conducted as follows. First, the base inductance of sensing coil, L_{s1}, L_{s2} and L_{s3} was measured at 1.51 MHz, 1.76 MHz and 1.95 MHz respectively. Next we regulated the normal force F_z at z direction by increasing the pressure of hydraulic cylinder #1 from 0 to 110.4 kPa with a 6.90 kPa step size. At each normal force, the shear force F_x applied along x direction was swept from 0 to 20.7 kPa with a 6.90 kPa step size. According to calibration, the applied normal force ranged from 0 to 800 N and shear force (F_x) ranged from 0 to 130 N. The inductance change of each sensing coil was measured at each step at its specific excitation frequency mentioned above. The changes in inductance ($\Delta L_s/L_s$) as a function of F_z and F_x are plotted in Fig. 6. After that, shear force along y direction F_y was applied by rotating the prototype sensor clockwise by 90 degree. Then inductance change caused by F_z and F_y are also plotted in Fig. 6. Each calibration curve was obtained by 5 repetitive

This article has been accepted for publication in a future issue of this journal, but has not been fully edited. Content may change prior to final publication. Citation information: DOI 10.1109/TBME.2014.2386136, IEEE Transactions on Biomedical Engineering

measurements, the average relative inductive change for each data point was used to plot the calibration curves in Fig. 6. Error bars were not plotted because they were too small to be seen.

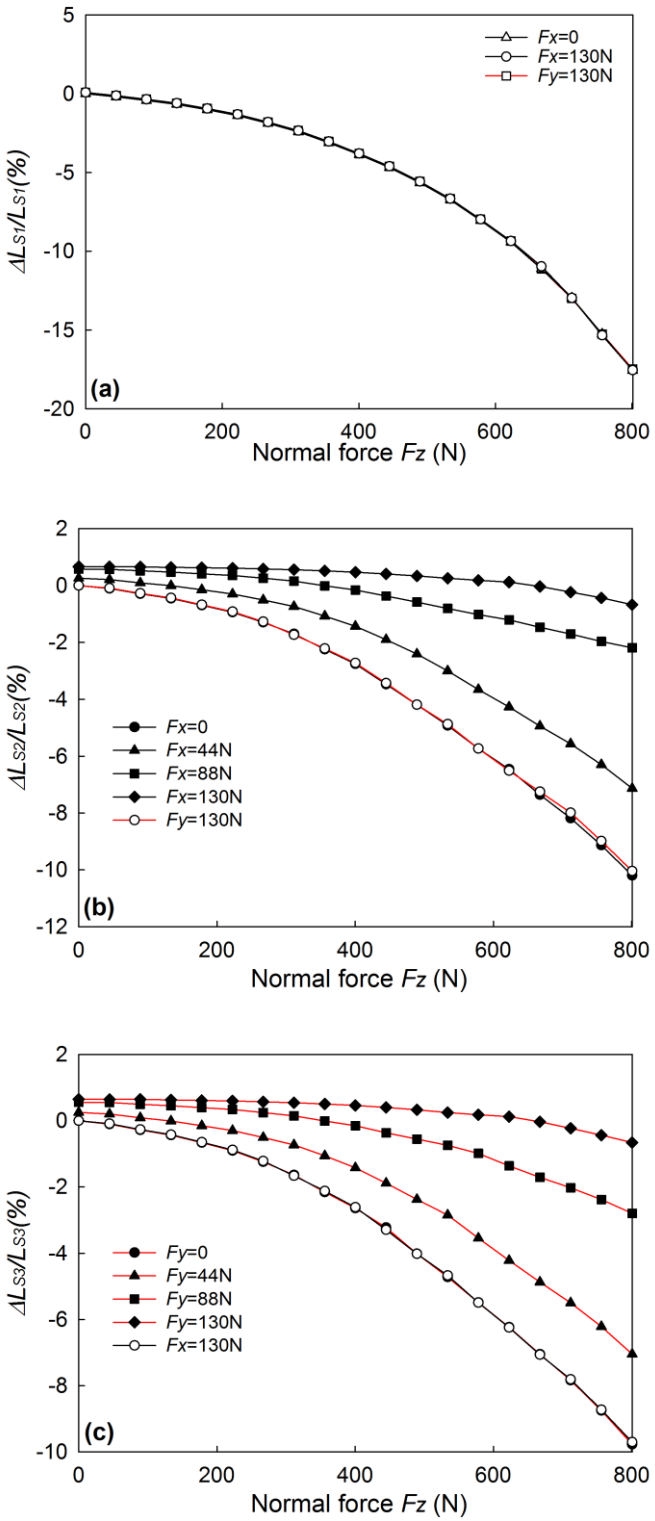

Fig. 6. Calibration curves for three sensing coils under various normal forces and shear forces. (a) Coil 1, (b) Coil 2, (c) Coil 3.

Fig. 6(a) illustrates the response of the central coil (Coil 1, to monitor normal force F_z). It is obvious the three curves under different shear forces are nearly identical. The applied normal force, F_z, caused a significant decrease in L_{s1} while shear force F_x and F_y up to 130 N had negligible effect on L_{s1}. This is because coil 1 was located at the center area; L_{s1} was only sensitive to the change in Z_d. Hence the F_z can be determined from Fig. 6(a) regardless of shear forces in x and y directions. For sensing coil 2 (located at the edge to monitor x-axis shear force F_x), Fig. 6(b) shows L_{s2} is dependent on both normal force F_z and x-axis shear force F_x, but insensitive to y-axis shear force F_y (red curve with circles in Fig. 6(b)). To determine shear force F_x, normal force should be determined first from coil 1's response; then F_x can be determined from calibration curves in Fig. 6(b). Similarly, shear force F_y can be obtained from inductance change of L_{s3} (red curve in Fig. 6(c)) after the normal force is determined. Although the shear force results in a small change in Z_d, this deformation is much smaller than that caused by the normal force; therefore shear forces applied on the sensor cause negligible change in the inductance change of coil 1 as shown in Fig. 6(a). Hence the error in normal force measurement caused by the applied shear force is negligible.

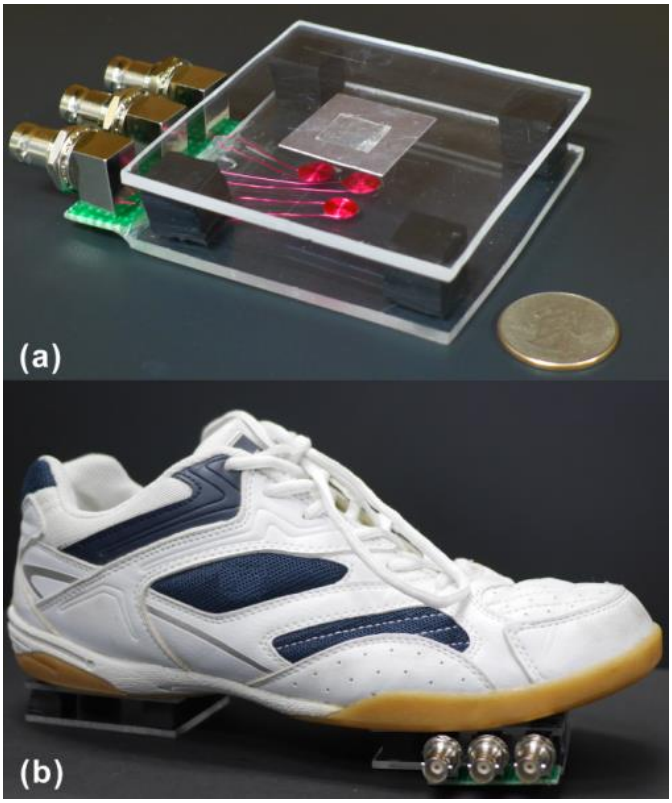

Fig. 7. Pictures of (a) the modified prototype sensor, and (b) a shoe with the modified prototype sensor attached at forefoot position.

B. *Dynamic testing*

To validate the sensor's capability of measuring dynamic normal force and shear forces in real time, the modified prototype sensor shown in Fig. 7a was tested during normal gait. The modified prototype sensor was attached at the forefoot and heel position of a right shoe separately via mounting tapes. Fig. 7b shows the shoe with the modified prototype sensor attached at forefoot position; a supporting structure with same size of the prototype sensor was attached at the heel position to keep

This article has been accepted for publication in a future issue of this journal, but has not been fully edited. Content may change prior to final publication. Citation information: DOI 10.1109/TBME.2014.2386136, IEEE Transactions on Biomedical Engineering

balance during walking. Four male volunteers were recruited to test the sensor. Informed consents were obtained prior to all experiments. First, a male subject with a weight of 716 N volunteered to test the prototype sensor. Male subject was asked to wear the modified shoe and walk normally to test the prototype sensor for 50 s. The first 10s and the last 10 s were excluded to obtain stable gait patterns.

To obtain the responses from the three sensing coils simultaneously with a single measurement, resonant frequency division multiplexing was applied to the signals from the three coils inductive sensor. A combination sinusoidal wave (10 V_{pp}, consisting of 1.51 MHz, 1.76 MHz and 1.95 MHz excitation signals) generated by an Agilent 33220A function generator was used to excite the three-coil inductive foot force sensor. A Gage Razor CompuScope 14-bit Multi-channel Digitizer was used to measure and record the voltage output (V_{out}) at a 100 MHz sampling rate in all experiments. Once the voltage output was recorded, the data was then processed in Matlab® to calculate the inductive changes for each sensing coil. The detailed signal processing procedures can be found in references [19, 20]. Finally, the inductance changes for three sensing coils were calculated and plotted in Fig. 8.

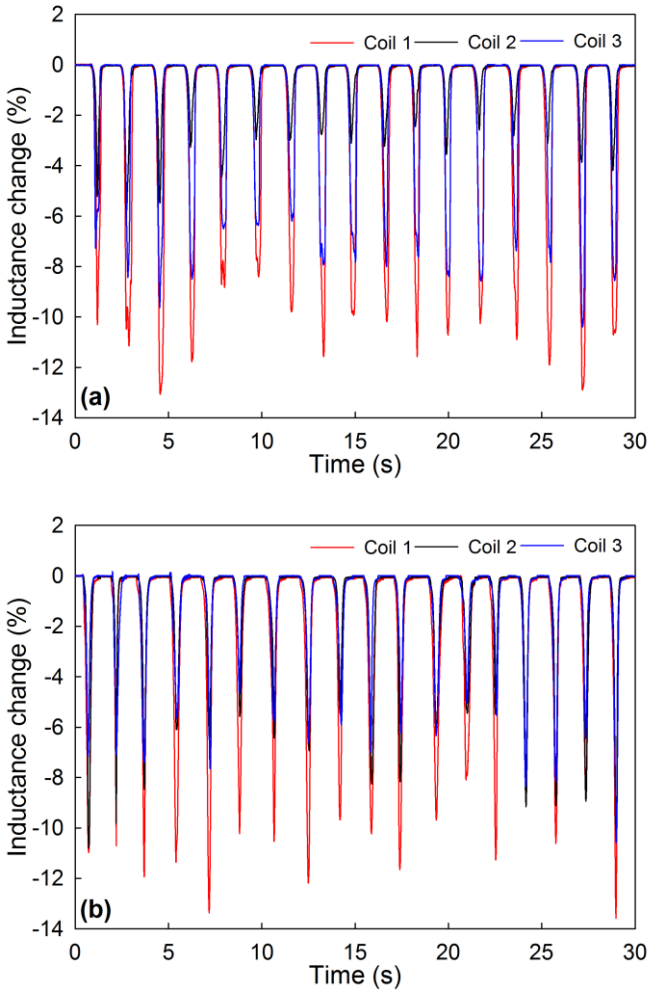

Fig. 8. Measured relative inductance changes of the three sensing coils during normal walking of a 716 N male subject, (a) Forefoot position, (b) Heel position.

The modified prototype sensor was tested in forefoot position and heel position separately. Fig. 8(a) illustrates the sensor's typical response at forefoot position. 17 negative inductive pulses were observed for each sensing coil. The time interval between adjacent negative inductive pulses represents one whole gait cycle, initiated with a landing phase, followed by a contacting phase and ended with a lifting phase. The average gait cycle is 1.67 s. The duration of each pulse was in the range of 0.74 s to 0.85 s. Fig. 8(b) shows the sensor's typical response at heel position measured in a separate experiment. 18 negative inductive pulses were observed for each sensing coil. The time interval between adjacent negative inductive pulses represents one whole gait cycle, initiated with a heel strike, followed by a mid-stance, push off and ended with a toe off. The average gait cycle is 1.58 s. The duration of each pulse was in the range of 0.71 s to 0.84 s.

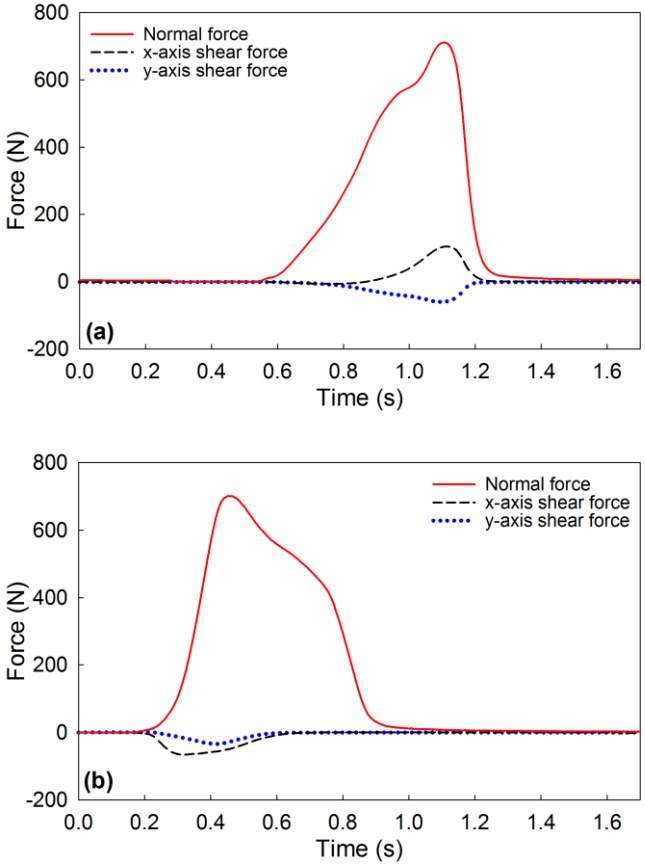

Fig. 9. Typical normal force and shear forces during one gait cycle for the 716 N male subject calculated from sensor responses, (a) Forefoot position, (b) Heel position.

Next the exact normal force and two axis shear forces were calculated by the following procedures: 1) normal force F_z was determined by the inductance change of coil 1 using the calibration curve shown in Fig. 6(a); 2) with the determined normal force, shear forces F_x and F_y were determined from the responses of coil 2 and coil 3 using calibration curves in Figs. 6(b) and 6(c). Fig. 9(a) illustrates the recovered typical normal force and shear forces at forefoot position during one gait cycle. As shown in Fig. 9(a), the duration of a typical gait cycle was approximately 0.79 s. A typical normal force generated in the

This article has been accepted for publication in a future issue of this journal, but has not been fully edited. Content may change prior to final publication. Citation information: DOI 10.1109/TBME.2014.2386136, IEEE Transactions on Biomedical Engineering

gait cycle (red solid curve in Fig. 9(a)) reached 712 N by the 716 N male subject, which matched the subject's body weight well. Black curve and blue curve in Fig. 9 indicate the generated *x*-axis (anteroposterior (AP)) shear force and *y*-axis (mediolateral (ML)) shear force, respectively. Negative AP shear force (posterior direction) was observed for heel (black dash curve in Fig. 9(b)) and positive AP shear force (anterior direction) was observed for forefoot (black dash curve in Fig. 9(a)). During the gait cycle, only negative ML shear force was observed, indicating the ML shear force was always along medial direction (blue dot curve in Fig. 9(a) and Fig. 9(b)). The measured waveforms and magnitudes of normal force, AP shear force and ML shear force shown in Fig. 9 are in good agreements with other studies on foot force measurements [13, 21].

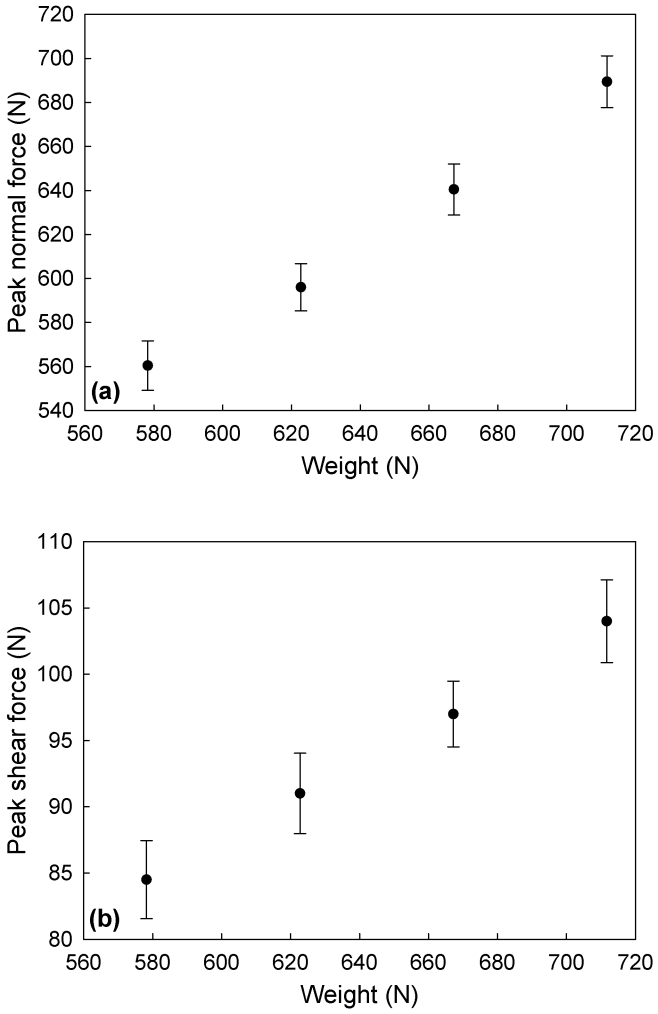

Fig. 10. Calculated peak force for four male subjects (580 N, 623 N, 667 N and 716N), (a) Normal force, (b) AP shear force.

Studies show most of the foot ulceration are developed at forefoot position [3]. This is because in a gait cycle the peak normal force and shear force both occur at forefoot position. Hence accurate detection of the peak value of normal and shear forces are critical for preventing foot ulceration. To further demonstrate the sensor's capability of detecting peak forces, we conducted experiments for four male subjects with different weights (580 N, 623 N, 667 N and 716 N). For each subject, 30 s data during gait was collected and processed to obtain peak forces at the forefoot position. The calculated peak normal forces and peak shear forces are plotted in Fig. 10(a) and Fig. 10(b), respectively. It is obvious the peak normal force for each subject is approximately equal to the subject's weight; and the peak shear force in *x*-direction is about 15% of the subject's weight; the peak shear force in *y*-direction is approximately half of the shear force in the *x*-direction. These measurements results agree well with prior results for normal walking reported by Mori and Marasovic [13, 22]. The tests proved that present sensor provides repeatable measurements of normal forces and shear forces on a foot.

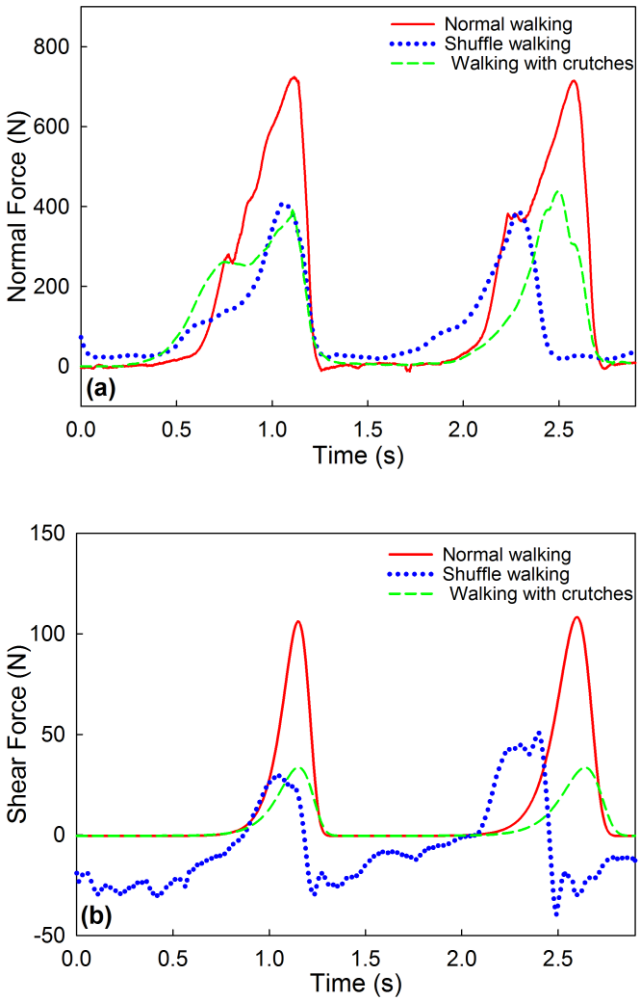

Fig. 11. Calculated normal force for three different gait patterns of a 716 N male subject. (a) Normal force, (b) AP shear force.

In addition, the prototype sensor was tested for three different gait patterns of a 716 N male subject, i.e., normal walking, walking with right foot shuffling and walking with crutches (three-point sequence, no-weight-bearing at left foot). Fig. 11(a) and Fig. 11(b) show the typical normal forces and AP shear forces for the three different gait patterns, respectively. In all experiments, the prototype sensor was installed at the forefoot position of the subject's right foot. Results clearly show the normal walking generated the largest peak of normal

This article has been accepted for publication in a future issue of this journal, but has not been fully edited. Content may change prior to final publication. Citation information: DOI 10.1109/TBME.2014.2386136, IEEE Transactions on Biomedical Engineering

force and shear force (red solid curve in Fig. 11). This is because during normal walking the peak forces occurred at the push off phase and the whole weight of the subject was applied on forefoot at push off phase. While for shuffle walking (blue dot curve in Fig. 11) and walking with crutches (green dash curve in Fig. 11), the whole weight of the subject was supported by both the forefoot and the heel when the right foot was pushed off the ground; hence the normal forces and shears forces measured at the forefoot position were reduced for both the two gait patterns. When the subject walked with right foot shuffling, a small positive normal force was observed during the shuffling phase (before the push off phase) because the right foot was still in contact with the ground. In addition, negative AP shear force was generated when the subject shuffled the right foot ahead and positive AP shear force was observed during the push off phase. In comparison, for normal walking and walking with crutches, normal and AP shear forces were zero when the right foot had no contact with the ground (swing phase), and were only generated at stance phase, i.e., from heel strike to toe off. The measurement results with the three different gait patterns agree very well with similar studies reported in [13] and [23]. This test shows the prototype senor can measure the differences in forces caused by gait patterns.

Note that although the prototype inductive foot force sensor is capable of accurately detecting the overall normal force and shear forces in real time, the spatial resolution of the measurement is low because of the large sensing area. This drawback can be overcome by decreasing the sensor size [3, 24]. With its simple structure, the sensor can be made much smaller (in millimeter level) and with lower cost using micro-fabrication techniques. Although we only tested a 76.2 mm ×76.2 mm ×16 mm prototype sensor at forefoot and heel position in our experiments for concept-demonstration purpose, more sensors with reduced sizes can be added for force measuring at various critical positions such as toes and five metatarsal heads (MTH) for force distribution measurement with high spatial resolution. With the use of resonance frequency division signal multiplexing/de-multiplexing [19], multiple miniature sensors/sensing coils can be embedded in the shoe of a diabetes patient for force monitoring at multiple positions with only one set of measurement, making the sensor suitable for force related foot ulceration monitoring with high spatial resolution.

IV. Conclusion

We demonstrated a multiplexed inductive sensor for ulcer related foot force monitoring. The sensor consists of three mini-sized planar coils. The normal forces and shear forces on a foot during walking were simultaneously measured by monitoring inductance changes of the three sensing coils. By applying the resonant frequency division multiplexing techniques, only one set of measurement circuit is required to measure normal force, AP and ML shear forces simultaneously. The use of resonant frequency division signal multiplexing enables high sensitivity and high resolution. Testing results demonstrated the simultaneous measurement of normal force ranging from 0 to 800 N and shear forces ranging from 0 to 130 N has been achieved. The signal multiplexing concept can be extended to multiple foot force sensors installed at multiple positions to provide a complete dynamic force measurement of the entire foot. With the extended capability, light weight and low cost, this sensor has a potential to be used for real time monitoring of the plantar forces to prevent foot ulceration.

Acknowledgment

This work is supported by the University of Akron. The authors thank Mr. Yu Han at the University of Akron for his assistance in conducting experiments.

References

[1] World Health Organization. (2009, Jun). Global health risks: Mortality and burden of disease attributable to selected major risks. Geneva, Switzerland. [Online]. Available: http://www.who.int/healthinfo/global_burden_disease/GlobalHealthRisks_report_full.pdf

[2] J. E. Perry, J. O. Hall and B. L. Davis. (2002, Feb). Simultaneous measurement of plantar pressure and shear forces in diabetic individuals. *Gait. Posture*. [Online]. *15(1)*, pp. 101-107. Available: http://www.gaitposture.com/article/S0966-6362(01)00176-X/pdf

[3] S.Ostadabbas et al. (2014, May). A knowledge based modeling for plantar pressure image reconstruction. *IEEE Trans. Biomed. Eng*. [Online]. *61(10)*, pp. 2538-2549. Available: http://ieeexplore.ieee.org/stamp/stamp.jsp?arnumber=6813648

[4] M. Yavuz, G. Botek and B. L. Davis. (2007, Apr). Plantar shear stress distributions: comparing actual and predicted frictional forces at the foot–ground interface. *J. Biomech*. [Online]. *40(13)*, pp. 3045-3049. Available: http://www.ncbi.nlm.nih.gov/pubmed/17449038

[5] M. Yavuz et al. (2007, Dec). Temporal characteristics of plantar shear distribution: relevance to diabetic patients. *J. Biomech*. [Online]. *41(3)*, pp. 556-559. Available: http://www.ncbi.nlm.nih.gov/pubmed/18054025

[6] N. Singh, D. G. Armstrong and A. L. Benjamin. (2005, Jan). Preventing foot ulcers in patients with diabetes. *J. AMER. MED. ASSOC*. [Online]. *293(2)*, pp. 217-228. Available: http://jama.jamanetwork.com/article.aspx?articleid=200119

[7] L. A. Lavery et al. (2007, Jan). Preventing diabetic foot ulcer recurrence in high-risk patients: use of temperature monitoring as a self-assessment tool. *Diabetes. Care*. [Online]. *30(1)*, pp. 14-20. Available: http://www.ncbi.nlm.nih.gov/pubmed/17192326

[8] B. Belmont et al. (2013, Mar). An apparatus to quantify anteroposterior and mediolateral shear reduction in shoe insoles. *J. Diabetes. Sci. Technol*. [Online]. *7(2)*, pp. 410-419. Available: http://www.ncbi.nlm.nih.gov/pubmed/23567000

[9] I. Mohammad and H. Huang. (2012, Jun). Plantar pressure sensing using loop antenna sensors. Presented at PETRA 2012. [Online]. Available: http://dl.acm.org/citation.cfm?id=2413107

[10] I. Mohammad, and H. Huang. (2012, Oct). Shear sensing based on a microstrip patch antenna. *Meas. Sci. Technol*. [Online]. *23(10)*. Available: http://iopscience.iop.org/0957-0233/23/10/105705

[11] A. A. Kalamdani, "Development and characterization of a high-spatial-temporal-resolution foot-sole-pressure measurement system," Ph. D. dissertation, Robotics. Institute., Carnegie Mellon Univ., Pittsburgh, United States, 2006.

[12] T. Bernard et al. (2009, Apr). An early detection system for foot ulceration in diabetic patients. Presented at IEEE 35th Annual Northeast conference. [Online]. Available: http://ieeexplore.ieee.org/xpls/abs_all.jsp?arnumber=4967797&tag=1

[13] T. Mori et al. (2012, Jun). Insole-Type Simultaneous Measurement System of Plantar Pressure and Shear Force during Gait for Diabetic Patients. *J. Robot. Mechatronics*. [Online]. *24(5)*, pp. 766-772. Available: http://www.rounenkango.m.u-tokyo.ac.jp/pdf/jrm_24_5_insole_type.pdf

[14] B. L. Davis et al. (1998, Feb). A device for simultaneous measurement of pressure and shear force distribution on the plantar surface of the foot. *J. Appl. Biomech*. [Online]. *14(1)*, pp. 93-104. Available: http://journals.humankinetics.com/jab-back-issues/jabvolume14issue1february/adeviceforsimultaneousmeasurementofpressureandshearforcedistributionontheplantarsurfaceofthefoot

[15] I. Mohammad and H. Huang. (2012, Mar). Pressure and shear sensing based on microstrip antennas. Presented at Sensors and Smart Structures Technologies for Civil, Mechanical, and Aerospace Systems 2012 conference. [Online]. Available: http://proceedings.spiedigitallibrary.org/proceeding.aspx?articleid=1314025

[16] M. J. Warren-Forward, R. M. Goodall and D. J. Pratt. (1992, Jan). Three-dimensional displacement and force transducer. *IEE. Proceedings-A*. [Online]. *139(1)*, pp. 21-29. Available: http://ieeexplore.ieee.org/stamp/stamp.jsp?arnumber=109685

[17] S. Rajala and J. Lekkala. (2014, May). Plantar shear stress measurements—A review. *Clinical. Biomech*. [Online]. *29(5)*, pp. 475-483. Available: http://www.sciencedirect.com/science/article/pii/S0268003314000941

[18] L. Du, X. Zhu and J. Zhe. (2014, Jun). A high sensitivity inductive sensor for blade tip clearance measurement. *Smart. Mater. Struct*. [Online]. *23(6)*. Available: http://iopscience.iop.org/0964-1726/23/6/065018

[19] L. Du et al. (2013, Jul). High throughput wear debris detection in lubricants using a resonance frequency division multiplexed sensor. *Tribol. Lett*. [Online]. *51(3)*, pp. 453-460. Available: http://link.springer.com/article/10.1007%2Fs11249-013-0179-x

[20] L. Du et al. (2013, Jul). Improving sensitivity of an inductive pulse sensor for detection of metallic wear debris in lubricants using parallel LC resonance method. *Meas. Sci. Technol*. [Online]. *24(7)*. Available: http://iopscience.iop.org/0957-0233/24/7/075106

[21] W. M. Chen et al. (2010, May). A novel gait platform to measure isolated plantar metatarsal forces during walking. *Meas. Sci. Technol*. [Online]. *43(10)*, pp. 2017-2021. Available: http://www.jbiomech.com/article/S0021-9290%2810%2900181-8/abstract

[22] T. Marasovic, M. Cecic, and V. Zanchi. (2009, Sep). Analysis and Interpretation of Ground Reaction Forces in Normal Gait. *WSEAS. T. Sc*. [Online]. *8(9)*, pp. 1105-1114. Available: http://www.wseas.us/e-library/transactions/systems/2009/29-755.pdf

[23] S. Li et al. (2001, Jan). Three-point gait crutch walking: variability in ground reaction force during weight bearing. *Arch. Phys. Med. Rehabil*. [Online]. *86(1)*, pp. 86-92. Available: http://www.ncbi.nlm.nih.gov/pubmed/11239291

[24] S. Urry. (1999, Jan). Plantar pressure-measurement sensors. *Meas. Sci.Technol*. [Online]. *10(1)*, pp. R16-R32. Available: http://iopscience.iop.org/0957-0233/10/1/017

Li Du received the M.S. degree in electrical engineering from Beijing University of Technology, China, in 2007, and the Ph.D. degree from the University of Akron in mechanical engineering, Akron, OH, USA, in 2012.

He is currently a postdoctoral research associate at mechanical engineering, University of Akron. His current research interests include microfluidic devices and MEMS sensors for health monitoring.

Xiaoliang Zhu received his M.S. degree in electrical engineering from Beijing University of Technology, China, in 2012. He is currently pursuing the Ph.D. degree in mechanical engineering at the University of Akron, Akron, OH, USA.

His research interests include design and fabricate MEMS devices for health monitoring.

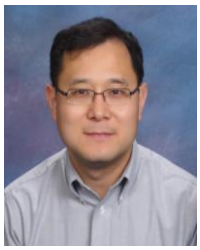

Jiang Zhe received his Ph.D. degree in mechanical engineering from Columbia University, New York, USA, in 2002.

Currently he is a professor in Mechanical Engineering at the University of Akron, Akron, OH, USA. His current research interests include microfluidic devices, lab-on-a-chip, and sensors for biomedical applications.